International Journal of Extreme Manufacturing

PAPER • **OPEN ACCESS**

GHz bursts in MHz burst (BiBurst) enabling high-speed femtosecond laser ablation of silicon due to prevention of air ionization

To cite this article: Kotaro Obata *et al* 2023 *Int. J. Extrem. Manuf.* **5** 025002

View the article online for updates and enhancements.

This content was downloaded from IP address 170.178.169.108 on 12/04/2023 at 08:59

OPEN ACCESS
IOP Publishing | IMMT
International Journal of Extreme Manufacturing
Int. J. Extrem. Manuf. 5 (2023) 025002 (7pp)
https://doi.org/10.1088/2631-7990/acc0e5

GHz bursts in MHz burst (BiBurst) enabling high-speed femtosecond laser ablation of silicon due to prevention of air ionization

Kotaro Obata[1], Francesc Caballero-Lucas[1], Shota Kawabata[1,2], Godai Miyaji[2] and Koji Sugioka[1,*]

[1] RIKEN Center for Advanced Photonics, 2-1 Hirosawa, Wako-shi, Saitama 351-0198, Japan
[2] Department of Applied Physics, Tokyo University of Agriculture and Technology, 2-24-16 Nakacho, Koganei, Tokyo 184-8588, Japan

E-mail: ksugioka@riken.jp

Received 30 March 2022, revised 30 August 2022
Accepted for publication 1 March 2023
Published 11 April 2023

Abstract

For the practical use of femtosecond laser ablation, inputs of higher laser intensity are preferred to attain high-throughput material removal. However, the use of higher laser intensities for increasing ablation rates can have detrimental effects on ablation quality due to excess heat generation and air ionization. This paper employs ablation using BiBurst femtosecond laser pulses, which consist of multiple bursts (2 and 5 bursts) at a repetition rate of 64 MHz, each containing multiple intra-pulses (2–20 pulses) at an ultrafast repetition rate of 4.88 GHz, to overcome these conflicting conditions. Ablation of silicon substrates using the BiBurst mode with 5 burst pulses and 20 intra-pulses successfully prevents air breakdown at packet energies higher than the pulse energy inducing the air ionization by the conventional femtosecond laser pulse irradiation (single-pulse mode). As a result, ablation speed can be enhanced by a factor of 23 without deteriorating the ablation quality compared to that by the single-pulse mode ablation under the conditions where the air ionization is avoided.

Keywords: BiBurst mode, GHz burst, laser ablation, silicon, air ionization

1. Introduction

Femtosecond laser ablation is well known for its ultrashort pulse width and extremely high peak intensity that provide superior performance in micro- and nano-processing of diverse materials [1–4]. Specifically, the ultrashort pulse width is shorter than the time for heat transfer from the electrons to the lattice, which can suppress the formation of heat-affected zone (HAZ) around laser ablated area, resulting in high-quality and high-precision fabrication at micro- and even nano-scales. In addition, the extremely high peak intensity can efficiently induce multiphoton absorption in materials, which transmit the laser beam, to process them with high-quality. As a result, femtosecond laser ablation is increasingly attracting attention for practical use in different applications. One of the important factors for the practical use of this ablation process is to improve throughput with no deterioration of ablation quality. However, several technical issues must be solved to achieve a high-throughput ablation process. Increasing the repetition rate of laser pulses is one solution. A repetition rate higher than several hundred kHz enhances the formation of HAZ

* Author to whom any correspondence should be addressed.

Original content from this work may be used under the terms of the Creative Commons Attribution 4.0 licence. Any further distribution of this work must maintain attribution to the author(s) and the title of the work, journal citation and DOI.

© 2023 The Author(s). Published by IOP Publishing Ltd on behalf of the IMMT

around the processed area due to the heat accumulation effect [2, 5]. Recently, femtosecond laser processing using a GHz burst mode has shown significant improvements in processing quality [6–17]. GHz burst mode of femtosecond laser pulses is composed of a group of laser pulse train with extremely short time intervals in a GHz frequency range. As a result, the energy supplied by the laser pulses can be deposited on the target material in a more temporally controlled manner as compared with the conventional irradiation scheme of femtosecond laser pulses (single-pulse mode). The first demonstration of GHz burst mode femtosecond laser ablation was implemented by Ilday's group [6]. They claimed that the target material is ablated before the heat generated by the laser pulses diffuses out of the processed area, such that most of the accumulated heat is removed along with the ablated material, known as ablation cooling for high-quality ablation with minimal thermal effects. They also showed that GHz burst mode ablation can improve ablation efficiency due to its efficient energy deposition (one order of magnitude higher). These results highly impacted the laser micro- and nano-processing community, and multiple research groups followed them to investigate GHz burst mode ablation [7–17]. Among them, we showed that GHz burst mode enhanced the ablation efficiency by a factor of 4.5 in femtosecond laser ablation of silicon at the laser intensities near ablation threshold as compared with the single-pulse mode when the same total energy was delivered [17].

Although ablation efficiency is one of the important factors for practical use, higher ablation rate per pulse is more critical to improving throughput. Higher ablation rates are generally achieved by using higher intensity. However, the higher intensity of femtosecond laser pulses often suffers from incidental damage due to air ionization and excessive heat generation [18, 19]. In this paper, we show that GHz burst mode ablation offers the possibility of overcoming these issues because the intensity of intra-pulses in the burst can be much lower than that of pulses in the conventional single-pulse mode ablation while achieving higher ablation efficiency. Looking ahead to more practical uses, we investigate the use of BiBurst mode, which is a combination of GHz bursts in MHz bursts, for ablation of silicon. We find that using single-pulse mode ablation at an intensity above the critical value damages the ablated surface due to air ionization. In contrast, BiBurst mode can deliver much higher total energy to ablate silicon without inducing air ionization due to its lower intra-pulse intensities. As a result, ablation speed can be increased by 23 times without degrading the ablation quality compared to that by the single-pulse mode ablation under the conditions that avoid the air ionization.

2. Experimental

Figure 1(a) shows an experimental setup for ablation using the femtosecond laser system with a BiBurst mode function. An Yb:KGW based high-power femtosecond laser system (Pharos, Light Conversion Ltd) delivered femtosecond laser pulses with a pulse duration of 220 fs at a near-infrared wavelength of 1030 nm. The maximum output power was 10 W. The laser pulses with good beam quality ($M^2 < 1.03$) oscillated from the femtosecond laser system propagated through some optical elements until reaching the sample surface placed on an XYZ stage to carry out ablation. The pulse energy was adjusted using polarizing optics composed of a $\lambda/2$ wave plate and a polarizing cubic beam splitter. The attenuated laser pulses with the original 2.5 mm-diameter Gaussian beam profile were focused through an objective lens of a numerical aperture of 0.4 onto the sample surface with a spot size of 3.8 μm in diameter at the beam waist. A p-type crystalline silicon wafer with 625 μm thickness, crystalline orientation (100), and conductivity of 3.11–3.41 Ω cm was used as the sample. To ensure the smallest laser beam spot size on the sample surface, an autofocusing system (ATF4, Wise Device Inc.) was used, in which a reference laser beam with a wavelength of 785 nm was introduced coaxially to the femtosecond laser beam to monitor the focused image with a CMOS sensor. After the laser beam passed through the $\lambda/2$ wave plate, the polarizing beam splitter reflected part of the beam to an ultrafast photodiode (ET-3500, Electro-Optics Technology Inc.) connected to an oscilloscope (Infiniivision DSOX6002A, Keysight Technologies Inc.) for imaging the temporal beam profile in the bursts.

Our configuration for the temporal evolution of the laser pulses used in this paper was bursts of pulses at a GHz repetition rate which were repeated at MHz to form a bigger packet of pulses, referred to as BiBurst mode. A detailed report of the operation of the BiBurst mode and the temporal distributions of the laser pulse energy in the BiBurst mode have been described in detail elsewhere [17]. To express the waveform of the BiBurst mode, we use the letter P to designate the number of pulses with a GHz repetition rate in the burst (intra-pulse number), and N for the number of bursts with a MHz repetition rate (burst number) (see figure 1(b) depicting the waveform of $N = 5$ and $P = 10$). The time separation between intra-pulses in the burst was 205 ps, which corresponded to a repetition rate of 4.88 GHz, so called GHz burst mode. The time separation between bursts was 15.6 ns, corresponding to a burst repetition rate of 64 MHz to generate the MHz burst mode. Although the MHz burst is typically repeated at hundreds kHz to generate the BiBurst mode, the number of MHz burst (packet) was fixed at 1 in this experiment. Ablation experiments using crystalline silicon were performed at N of 1, 2, and 5 with P of 1, 2, 5, 10 15, and 20 ($P = 1$ corresponds to single-pulse mode). Entire N bursts in series, each containing P intra-pulses, were termed the pulse packet. To properly compare the different burst mode configurations, results were evaluated by the packet energy E_{packet}, which is given by

$$E_{\text{packet}} = (E_{\text{intra-pulse}} \times P) \times N,$$

where $E_{\text{intra-pulse}}$ is the energy of the intra-pulses in the GHz burst, and ($E_{\text{intra-pulse}} \times P$) corresponds to the burst energy. Energy of each intra-pulse was adjusted to be almost constant.

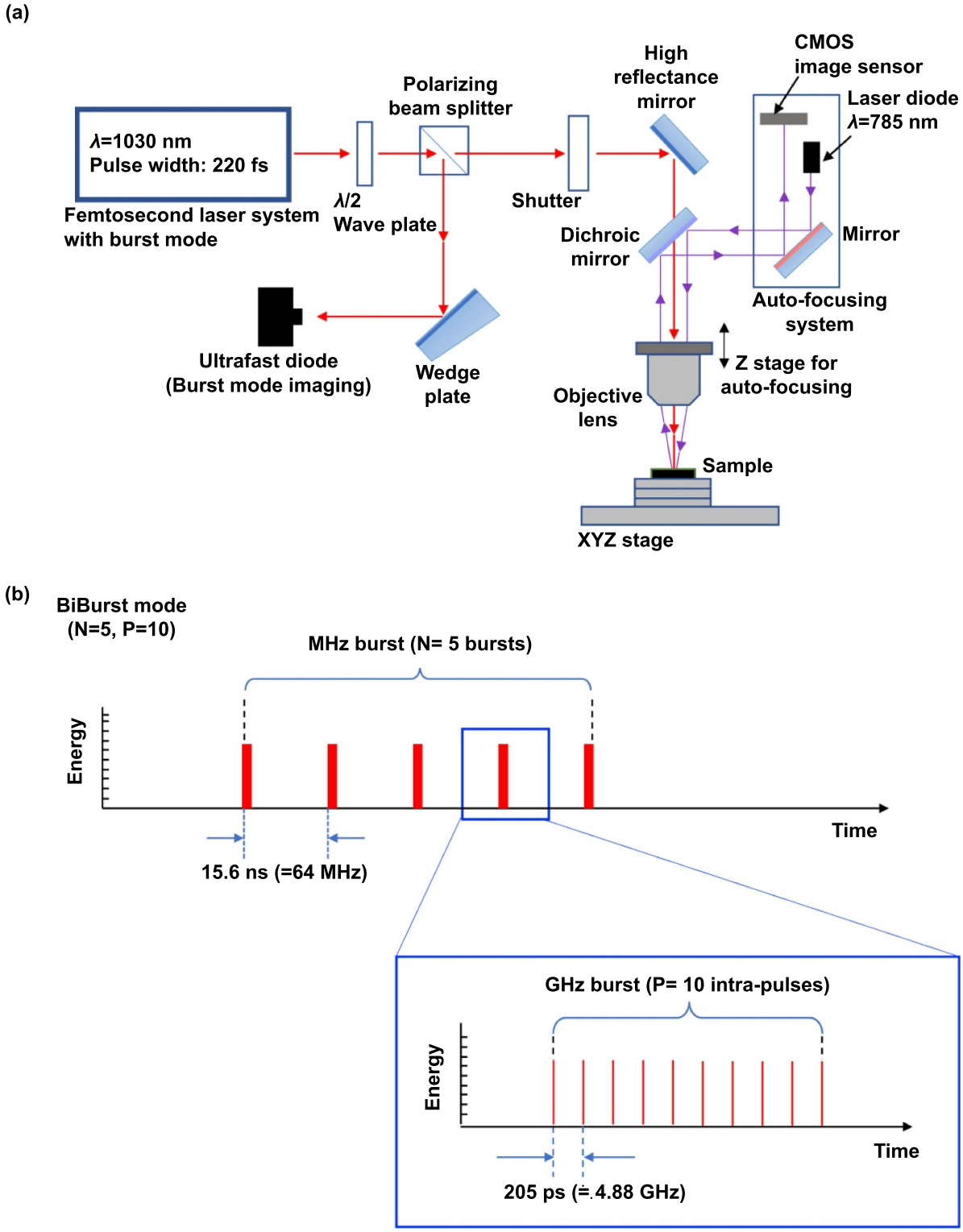

Figure 1. Schematic illustration of (a) the experimental setup for the GHz BiBurst mode femtosecond laser ablation and (b) pulse form of BiBurst mode, which represents 5 burst pulses with 64 MHz repetition rate (upper figure), each containing 5 intra-pulses with 4.88 GHz repetition rate ($N = 5$, $P = 10$) (lower figure). The time intervals of MHz burst and GHz burst are kept constant at 15.6 ns (=64 MHz) and 205 ps (=4.88 GHz), respectively. All the experiments in this work were performed with a single packet (single shot of MHz burst).

However, the intensity of last pulse was 2.9 times higher than the average of others due to characteristics of the opto-mechanical configuration of laser system used in which the burst pulse trains were generated. From the waveform of 25 intra-pulses in the GHz burst measured using the ultrafast photodiode, the standard deviation of the intensities of first 24 intra-pulses was evaluated to be 0.053, when the mean value of each signal intensity was set at 1.000.

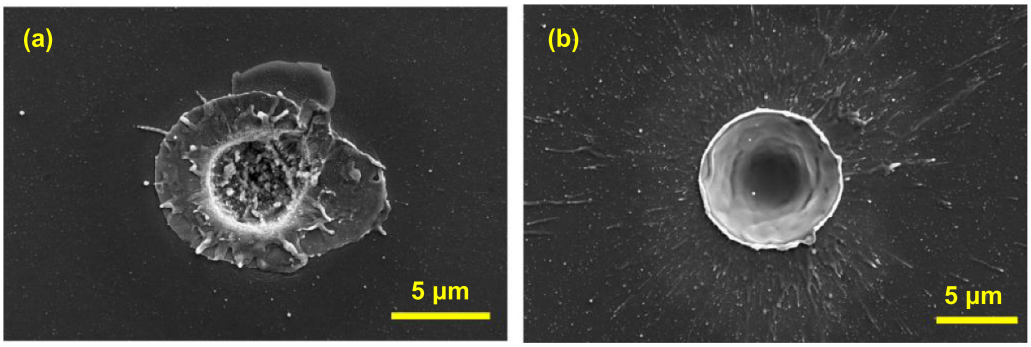

Figure 2. SEM images of ablated spots on the silicon surfaces with different configurations: (a) single-pulse mode ($N = 1$, $P = 1$) and (b) BiBurst mode ($N = 5$, $P = 20$) (5 bursts with 20 intra-pulses per burst). Packet energy was set at 12.8 μJ for the both cases.

Scanning electron microscopy (SEM) was used to observe the morphology of the ablated spots. Ablation rate and efficiency were evaluated by measuring the dimensions of the ablated spots using a laser scanning microscopy (LSM).

3. Results and discussion

Figure 2 shows SEM images of the ablated spot created by (a) single-pulse mode ($N = 1$, $P = 1$, single shot of femtosecond laser pulse) and (b) BiBurst mode with 5 bursts containing 20 intra-pulses ($N = 5$, $P = 20$). The packet energy was set at 12.8 μJ for both cases for a proper comparison of the different configurations. For single-pulse mode ablation, the surface of the ablated crater shows severe roughness compared with the surface of the non-irradiated substrate. The roughness induced by single-pulse mode ablation is much more significant than that of the ablation in our previous work, which had a much lower packet energy of 0.53 μJ [17]. Severe roughness may be partially due to excess heat generation under this high laser intensity condition. More significantly, air ionization around the focus position of the laser beam was visually observed during the experiment. Specifically, when the sample position was moved towards the objective lens along the beam axis by using a Z-stage, ablation did not take place. However, the emission from air ionization was clearly observed at the laser focus point. Therefore, generated plasma should interact with the substrate to roughen the surface. Importantly, the maximum pulse energy for the single-pulse mode where the ablated profile can be measured by LSM is 3 μJ (see figure 4(a)), which corresponds to the peak intensity of 2.4×10^{14} W cm^{-2}. Above this critical peak intensity, the air ionization is considered to be induced, since it is sufficiently high to induce the air ionization via multiphoton ionization and tunnel ionization [20]. Meanwhile, the peak intensities for BiBurst shown in figures 4–6 are smaller than this critical value. In addition, the large area surrounding the ablated crater is covered with melted materials. Therefore, single-pulse mode ablation with high laser intensity has detrimental effects on the surface quality for practical use. Meanwhile, figure 2(b) shows the ablated crater fabricated by the BiBurst ($N = 5$, $P = 20$) at the same packet energy (12.8 μJ) as that of the single-pulse mode shown in figure 2(a). The same

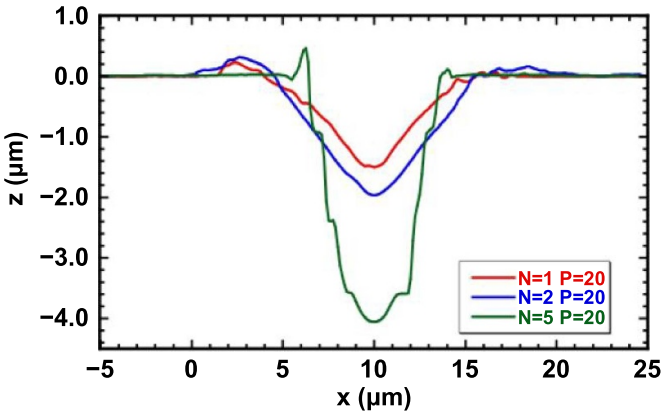

Figure 3. Cross-sectional profiles of the craters ablated by BiBurst mode at different burst numbers ($N = 1, 2, 5$) with same intra-pulse numbers ($P = 20$), which were measured by LSM.

packet energy means that the intra-pulse energy for BiBurst is 1/100 of the pulse energy for single-pulse mode. The ablated spot fabricated by BiBurst mode is well defined with a smooth surface and no signs of air ionization. Deposition of melted materials around the ablated area is less obvious. Importantly, the quality of ablated surface is similar to the surface created at lower packet energies [17]. The smooth surface achieved by GHz BiBurst mode should be responsible for gentle heating induced by the successive energy deposition [7]. Additionally, the intra-pulse energy, which was significantly lower than the pulse energy of single-pulse mode, prohibited air ionization to achieve the high-quality ablated surface.

To get more information on the dimensions of the ablated craters, the deepest points of the cross-sectional profiles were measured by LSM, as shown in figure 3. All samples were fabricated at the same packet energy of 12.8 μJ at different burst numbers ($N = 1, 2, 5$) with same intra-pulse numbers ($P = 20$). BiBurst mode ablation with larger burst numbers produces deeper craters. Interestingly, 5 bursts ($N = 5$) create a significantly deeper crater while a narrower diameter. These tendencies associated with the burst number for the same packet energy are consistent with the results obtained at a lower energy [17]. The profile of the crater ablated by single-pulse mode at a pulse energy of 12.8 μJ is shown in

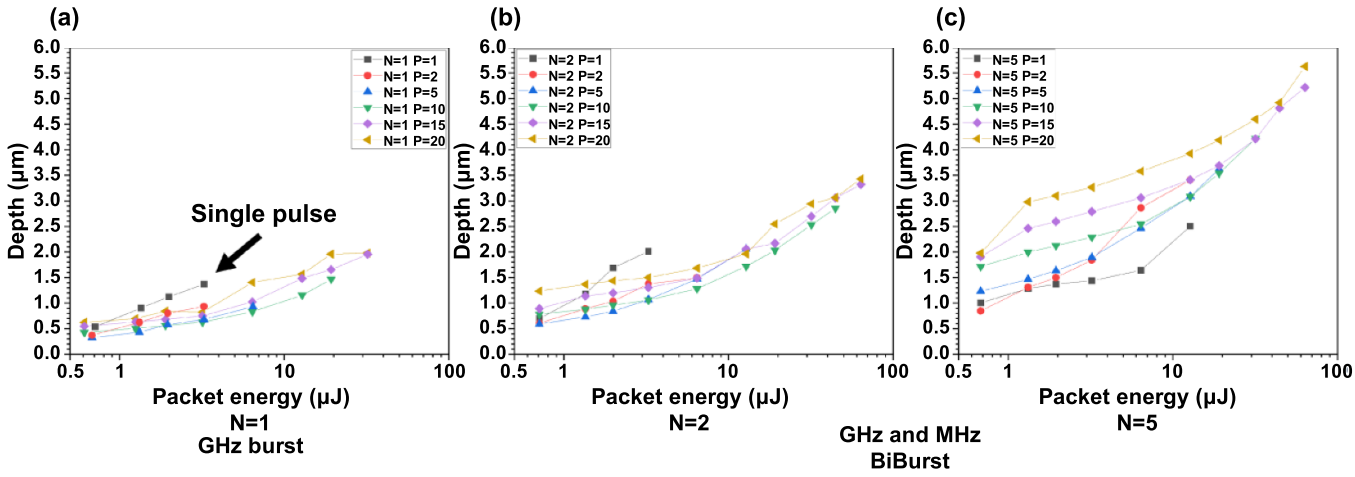

Figure 4. Dependence of ablated depth measured by LSM on the packet energy delivered for the different burst mode configurations (Intra-pulse number P of 1, 2, 5, 10, 15, and 20: (a) single burst ($N = 1$), BiBurst modes (b) with $N = 2$ and (c) with $N = 5$).

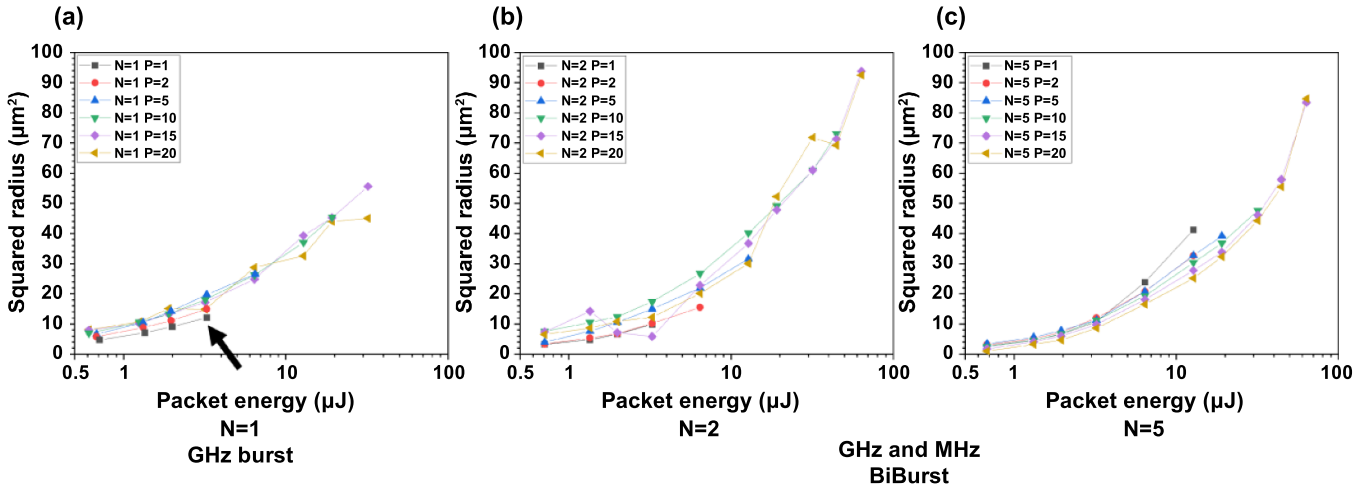

Figure 5. Dependence of squared radius of the ablated craters measured by LSM on the packet energy delivered for the different burst mode configurations (Intra-pulse number P of 1, 2, 5, 10, 15, and 20: (a) single burst ($N = 1$), BiBurst modes (b) with $N = 2$ and (c) with $N = 5$).

figure 7. The ablated surface was heavily roughened as also confirmed in figure 2. Additionally, a spike structure higher than the depth of the crater was observed at the crater's center. However, such a spike structure was not found in figure 2. We consider that the SEM image gives more reliable information on exact structures. Therefore, we attribute the spike structure to heavy scattering of the LSM's incident light by the roughened surface, which disables the measurements of samples prepared at higher packet energies by the single-pulse mode.

For a more detailed investigation, the results obtained by measurements using the LSM are summarized in figures 4–6. Figures 4(a)–(c) show dependence of the ablated depth on the packet energy for the MHz burst numbers N of 1, 2, and 5, respectively, with the various intra-pulse numbers ($P = 1, 2, 5, 10, 15, 20$). For an easier comparison with single-pulse mode, the results obtained by ablation with a single pulse of femtosecond laser ($N = 1, P = 1$) is highlighted with the black arrow in figure 4(a). For a single shot of burst ($N = 1$, figure 4(a)), the GHz burst mode does not create deeper craters than the single-pulse mode ablation at the same packet energy higher than 0.7 μJ. In contrast, our previous work showed that the GHz burst mode ablated deeper than the single-pulse mode at an energy below 0.7 μJ [17]. This result might be attributed to ablation efficiency. Specifically, the ablation efficiency of GHz burst is higher than that of single-pulse mode at the lower packet energy. The maximum ablation efficiency can be attained for the intra-pulse energy below the ablation threshold pulse energy by the single-pulse mode. The enhanced ablation efficiency is due to collaborative contribution of successive intra-pulses. Specifically, preceding intra-pulses in the burst produce transient absorption sites for the succeeding intra-pulses due to free electron generation to enhance the ablation efficiency. However, the efficiency gradually decreases as the intra-pulse energy exceeds the threshold, because individual intra-pulses can directly induce ablation. The collaborative contribution of successive intra-pulses is no longer expected in this regime. For $N = 2$ (figure 4(b)), the depth obtained at the lower packet energy by BiBurst is deeper than that by single-pulse mode, while it is reversed at the higher

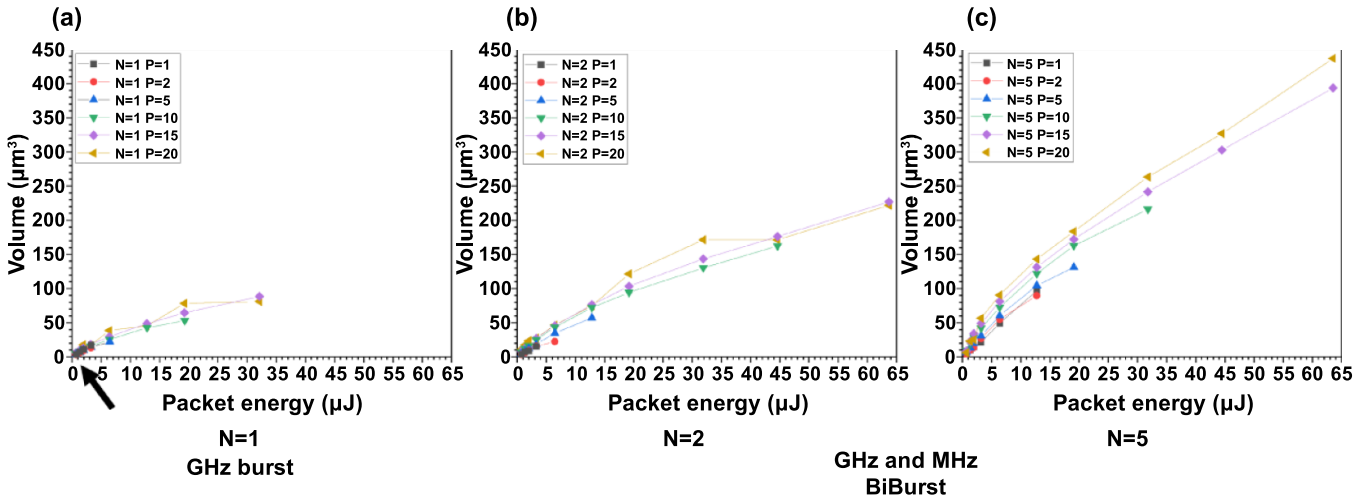

Figure 6. Dependence of the volume of ablated craters measured by LSM on the packet energy delivered for different burst mode configurations (Intra-pulse number P of 1, 2, 5, 10, 15, and 20: (a) single burst ($N = 1$), BiBurst modes (b) with $N = 2$ and (c) with $N = 5$).

packet energy due to increase of intra-pulse energy beyond the ablation threshold. For $N = 5$, the intra-pulse energy of BiBurst is still low enough to achieve higher ablation efficiency than the single-pulse mode, resulting in deeper craters. Larger P gives deeper depth due to lower intra-pulse energy, in other words, higher ablation efficiency. More importantly, the ablated craters produced by the single-pulse mode at the pulse energy above the critical value were not able to be measured by the LSM because of the heavy surface roughness produced by air ionization, as shown in figure 7. Such low-quality surfaces are not suitable for practical use. Even for BiBurst mode, air breakdown is generated to deteriorate the quality when the intra-pulse energy exceeds the critical value, where the depth cannot be measured by LSM due to heavy scattering by the roughened surfaces similarly to the single-pulse mode. However, for larger P that makes the intra-pulse energy smaller than the critical value, the depth ablated by BiBurst monotonically increases as the packet energy increases with no influence from air ionization.

Here, as another factor of dimensions of ablated craters, the squared radius of ablated craters corresponding to figures 4(a)–(c) are mapped in figures 5(a)–(c), respectively. For a single shot of GHz burst ($N = 1$, figure 5(a)), larger areas are ablated at the same packet energy as compared with the single-pulse mode. This is due to the Burst's reduced threshold energy, since lower threshold energy usually produces larger ablation spots, according to the threshold effect [21]. For BiBurst mode ($N = 2$, figure 5(b) and $N = 5$, figure 5(c)), the ablated areas are comparable to or slightly smaller than those of the single-pulse mode. We also observed similar trends at the lower packet energy, for which we concluded that the balance between the reduction of the threshold energy and the lower energy carried by each intra-pulse determines the resulting ablated area for the Burst mode [17].

In order to obtain a complete view of the ablation efficiency, which is one of the most important parameters for practical use, ablated volumes of craters corresponding to figures 4 and 5 were evaluated by LSM, as shown in figures 6(a)–(c). For

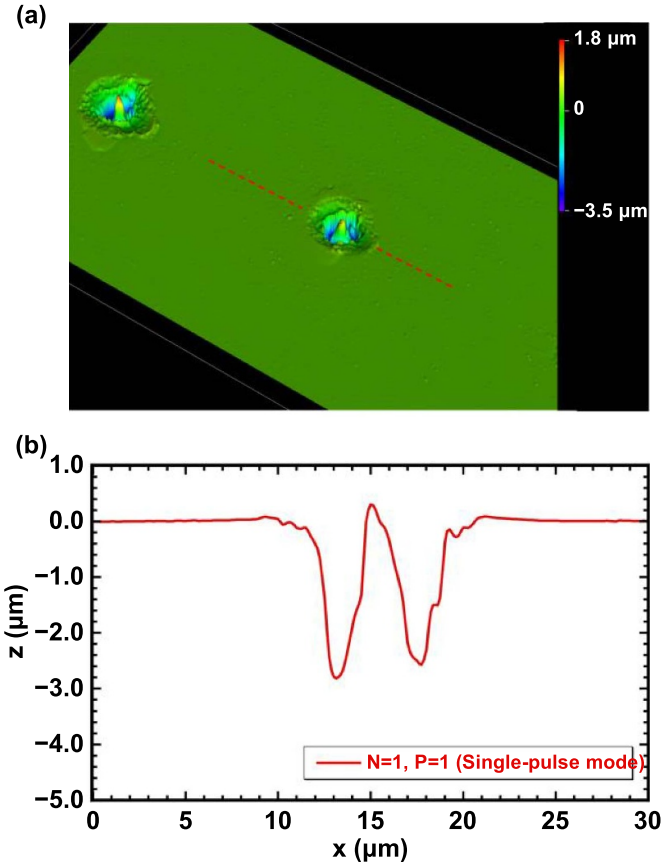

Figure 7. (a) 3D image and (b) cross-sectional profile of craters ablated on the silicon surface by a single pulse irradiation of femtosecond laser with a pulse energy of 12.8 μJ (single-pulse mode, $N = 1$, $P = 1$), which was measured by LSM.

each configuration with different burst pulse numbers ($N = 1$, 2, 5), the burst mode ablation can ablate larger volumes at the same packet energy as compared with the single-pulse mode ablation, indicating enhanced ablation efficiency. Improvement in ablation efficiency becomes more pronounced as N

and P increase due to lower intra-pulse energy. Comparing the largest volumes obtained by the different ablation modes without air ionization, the BiBurst mode ($N = 5$, $P = 20$, $E_{\text{packet}} = 63.7\ \mu$J) can ablate a volume 23 times larger than that by single-pulse mode ablation ($N = 1, P = 1, E_{\text{packet}} = 3.3\ \mu$J) under the current experimental conditions.

4. Conclusion

To explore the capability of high-speed processing by BiBurst mode for practical use, the influence of ablation efficiency for crystalline silicon samples was investigated at significantly higher packet energy in different configurations of the burst modes. The controlled energy deposition on silicon during irradiation with multiple intra-pulses in the burst improved ablation efficiency as compared with the single-pulse mode when the same packet energy was delivered. The single-pulse mode ablation severely roughened ablated surfaces due to air ionization and excess heat generation when the pulse energy exceeded a critical value, which made it no longer applicable to practical use. In contrast, BiBurst mode ablation with larger P was able to avoid air ionization due to decreased intra-pulse energy, so that much deeper craters were created even at the large packet energy with little deterioration of ablation quality. Consequently, the BiBurst mode ablation showed 23 times higher ablation speed as compared with that by the single-pulse mode ablation under conditions that prevent air ionization. Thus, we can conclude that Biburst mode ablation has the potential to provide much higher throughput while maintaining high quality for practical use.

Acknowledgments

The authors would like to thank the Materials Characterization Support Unit, RIKEN CEMS for providing access to the SEM. This work was supported by MEXT Quantum Leap Flagship Program (MEXT Q-LEAP) Grant Number JPMXS0118067246.

ORCID iDs

Kotaro Obata https://orcid.org/0000-0003-3077-0527
Francesc Caballero-Lucas https://orcid.org/0000-0003-0335-9468
Shota Kawabata https://orcid.org/0000-0001-7938-7858
Godai Miyaji https://orcid.org/0000-0002-9079-4064
Koji Sugioka https://orcid.org/0000-0002-7174-5961

References

[1] Sugioka K and Cheng Y 2014 Ultrafast lasers—reliable tools for advanced materials processing *Light Sci. Appl.* **3** e149
[2] Sugioka K and Cheng Y 2014 Femtosecond laser three-dimensional micro- and nanofabrication *Appl. Phys. Rev.* **1** 041303
[3] Phillips K C, Gandhi H H, Mazur E and Sundaram S K 2015 Ultrafast laser processing of materials: a review *Adv. Opt. Photonics* **7** 684–712
[4] Nolte S, Schrempel F and Dausinger F 2016 *Ultrashort Pulse Laser Technology* vol 195 (Cham: Springer)
[5] Eaton S M, Zhang H B, Herman P R, Yoshino F, Shah L, Bovatsek J and Arai A Y 2005 Heat accumulation effects in femtosecond laser-written waveguides with variable repetition rate *Opt. Exp.* **13** 4708–16
[6] Kerse C *et al* 2016 Ablation-cooled material removal with ultrafast bursts of pulses *Nature* **537** 84–88
[7] Mishchik K, Bonamis G, Qiao J, Lopez J, Audouard E, Mottay E, Hönninger C and Manek-Hönninger I 2019 Highefficiency femtosecond ablation of silicon with GHz repetition rate laser source *Opt. Lett.* **44** 2193–6
[8] Bonamis G, Audouard E, Hönninger C, Lopez J, Mishchik K, Mottay E and Manek-Hönninger I 2020 Systematic study of laser ablation with GHz bursts of femtosecond pulses *Opt. Exp.* **28** 27702–14
[9] Metzner D, Lickschat P and Weißmantel S 2020 High-quality surface treatment using GHz burst mode with tunable ultrashort pulses *Appl. Surf. Sci.* **531** 147270
[10] Hodgson N, Allegre H, Starodoumov A and Bettencourt S 2020 Femtosecond laser ablation in burst mode as a function of pulse fluence and intra-burst repetition rate *J. Laser Micro Nanoeng.* **15** 236–44
[11] Metzner D, Lickschat P and Weißmantel S 2021 Optimization of the ablation process using ultrashort pulsed laser radiation in different burst modes *J. Laser Appl.* **33** 012057
[12] Žemaitis A, Gaidys M, Gečys P, Barkauskas M and Gedvilas M 2021 Femtosecond laser ablation by bibursts in the MHz and GHz pulse repetition rates *Opt. Exp.* **29** 7641–53
[13] Matsumoto H, Lin Z B, Schrauben J N and Kleinert J 2021 Ultrafast laser ablation of silicon with ∼GHz bursts *J. Laser Appl.* **33** 032010
[14] Obata K, Caballero-Lucas F and Sugioka K 2021 Material processing at GHz burst mode by femtosecond laser ablation *J. Laser Micro Nanoeng.* **16** 19–23
[15] Sugioka K 2021 Will GHz burst mode create a new path to femtosecond laser processing? *Int. J. Extrem. Manuf.* **3** 043001
[16] Förster D J, Jäggi B, Michalowski A and Neuenschwander B 2021 Review on experimental and theoretical investigations of ultra-short pulsed laser ablation of metals with burst pulses *Materials* **14** 3331
[17] Caballero-Lucas F, Obata K and Sugioka K 2022 Enhanced ablation efficiency for silicon by femtosecond laser microprocessing with GHz bursts in MHz bursts (BiBurst) *Int. J. Extrem. Manuf.* **4** 015103
[18] Zhang H, Zhang F T, Du X, Dong G P and Qiu J R 2015 Influence of laser-induced air breakdown on femtosecond laser ablation of aluminum *Opt. Exp.* **23** 1370–6
[19] Ancona A, Röser F, Rademaker K, Limpert J, Nolte S and Tünnermann A 2008 High speed laser drilling of metals using a high repetition rate, high average power ultrafast fiber CPA system *Opt. Exp.* **16** 8958–68
[20] Braun A, Korn G, Liu X, Du D, Squier J and Mourou G 1995 Self-channeling of high-peak-power femtosecond laser pulses in air *Opt. Lett.* **20** 73–75
[21] Garcia-Lechuga M, Utéza O, Sanner N and Grojo D 2020 Evidencing the nonlinearity independence of resolution in femtosecond laser ablation *Opt. Lett.* **45** 952–5